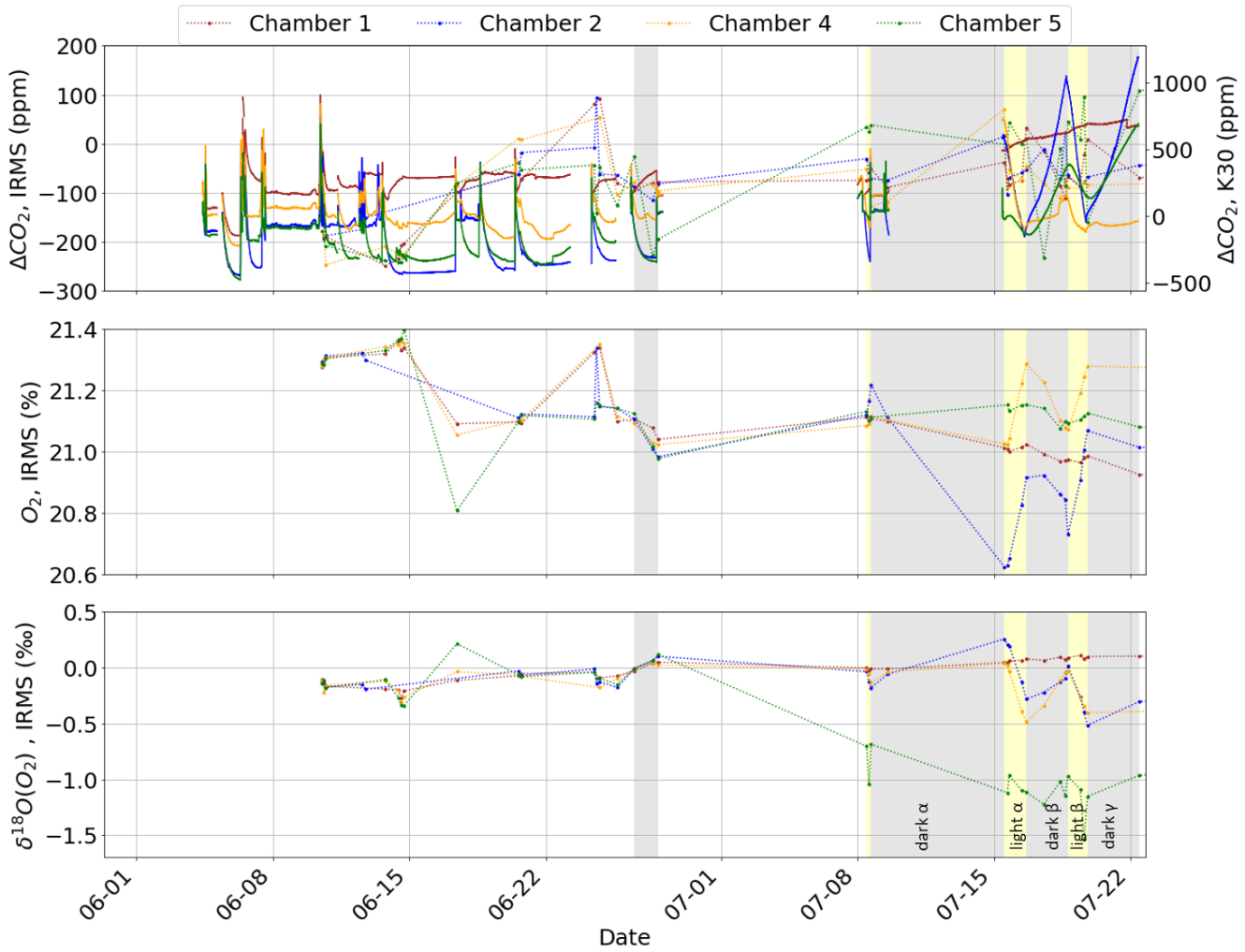


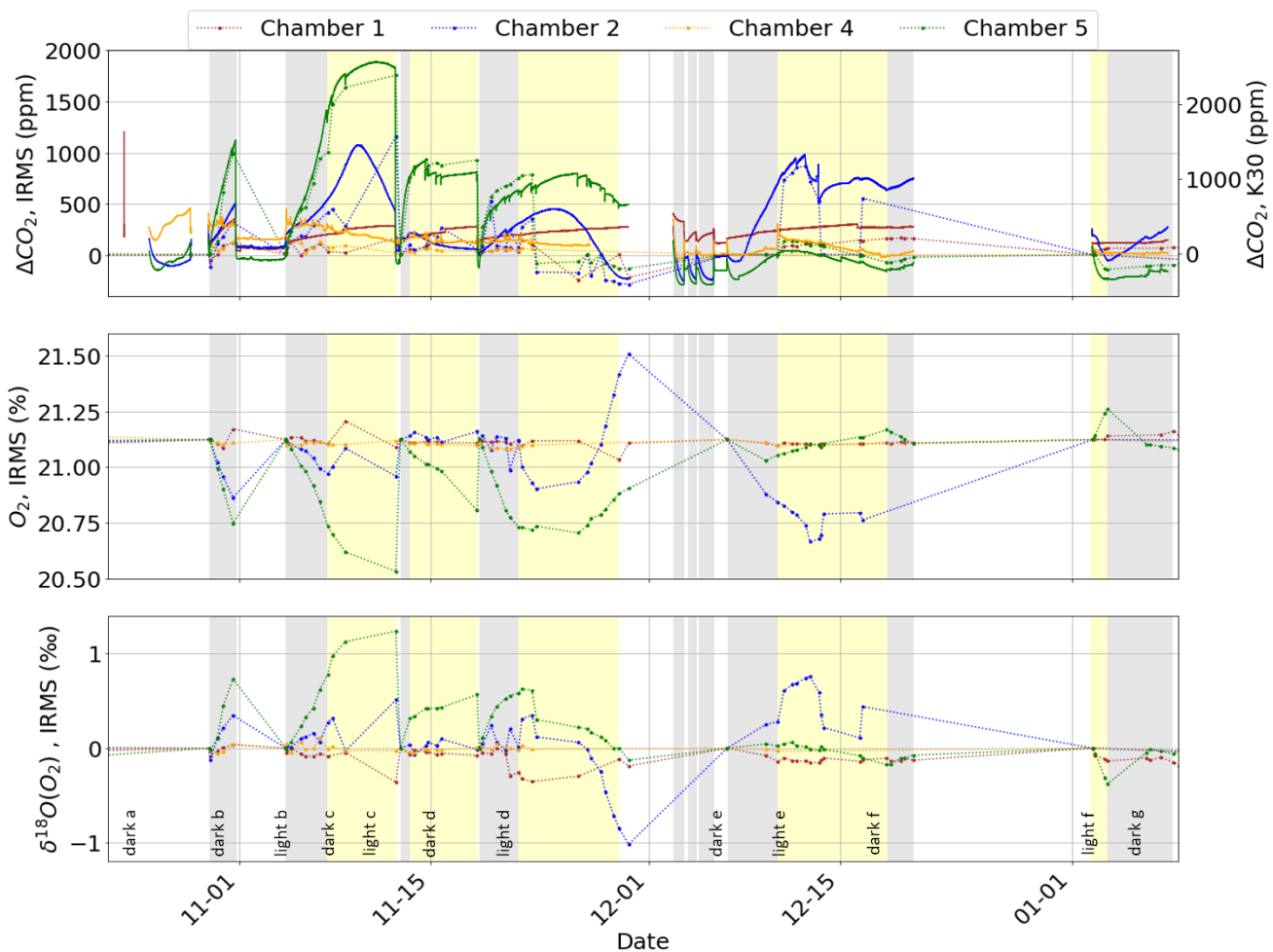
S1.Temporal evolution of CO₂ and O₂ elemental and isotopic compositions for the other batches of algae cultures

In Fig. S1, we present the results obtained for the first batch of algae culture. The initial trials were not working as expected as we were still adjusting crucial parameters: (1) time for the water system to arrive at equilibrium with the atmosphere before closing the chambers and beginning the experiment, (2) concentration of algae culture in order to have a signal strong enough to be measured. We also faced interruption in CO₂ sensor measurements caused by power cut-out. Eventually, on the last 4 phases (2 light and 2 dark) we managed to obtain a signal strong enough to be measured, and coherent with the expectations for photosynthesis and respiration dominated phases (especially for chambers 2 and 4). However, because of logistical issues (restricted access to the laboratory), we could not obtain frequent samples during each phase.



660 **Figure S1: Evolution of CO₂ concentration (top panel), O₂ concentration (middle panel) and $\delta^{18}\text{O}(\text{O}_2)$ (bottom panel) in 4 instrumented chambers. The horizontal axis represents time, with the plot beginning at the injection of osmosed water into the microcosm tube. Coloured vertical bands highlight the dark (in gray) and light (in yellow) phases, and the background stays white for indicating when the chambers have been opened in order to reset the atmosphere composition of the chambers. The CO₂ evolution is expressed as delta values with respect to atmospheric air. It was measured continuously by the uncalibrated K30 sensor inside the top-module (solid line, plotted against the right-side axis) and also discretely by IRMS from the flask samplings (dotted line, plotted against the left-side axis).**

In Fig. S2, we present the results obtained for the second batch of algae culture. The results were better than for the 1st batch presented in Fig. S1. All the crucial parameters were set, and we solved the logistics which allowed us to have more samples for each phase. However, we were surprised by the delay between the change in lighting and the change in CO₂ and O₂ concentration, which caused us to interrupt 2 measurement phases too soon. We also detected a leak in chamber 4 which explained why it was not showing any expected trends.



675 **Figure S2: Evolution of CO₂ concentration (top panel), O₂ concentration (middle panel) and δ¹⁸O(O₂) (bottom panel) in 4 instrumented chambers. The horizontal axis represents time, with the plot beginning at the injection of osmosed water into the microcosm tube. Coloured vertical bands highlight the dark (in gray) and light (in yellow) phases, and the background stays white for indicating when the chambers have been opened in order to reset the atmosphere composition of the chambers. The CO₂ evolution is expressed as delta values with respect to atmospheric air. It was measured continuously by the uncalibrated K30 sensor inside the top-module (solid line, plotted against the right-side axis) and also discretely by IRMS from the flask samplings (dotted line, plotted against the left-side axis).**

680

S2.Results obtained with the OF-CEAS analyser

In parallel with flask samplings for measurements with IRMS, we also measured O₂ concentration and δ¹⁸O(O₂) with the laser spectrometer characterised by Piel et al. (2024) and used by Paul et al. (2025). However, since we had a modified prototype (cavity pressure at 50mbar instead of 150mbar), we measured the new minimum of Allan deviation to be of about 600s instead of 200s for Piel et al. (2024). As a result, we used 10min average for data cleaning, and we had longer measurement periods. This instrument unfortunately had instability problems, and we could only use it for one chamber, and for a short period of 1 light phase and 1 dark phase. Figure S3 presents the results obtained for these 2 phases (light 5 and dark 6), and compares them to results obtained with IRMS.

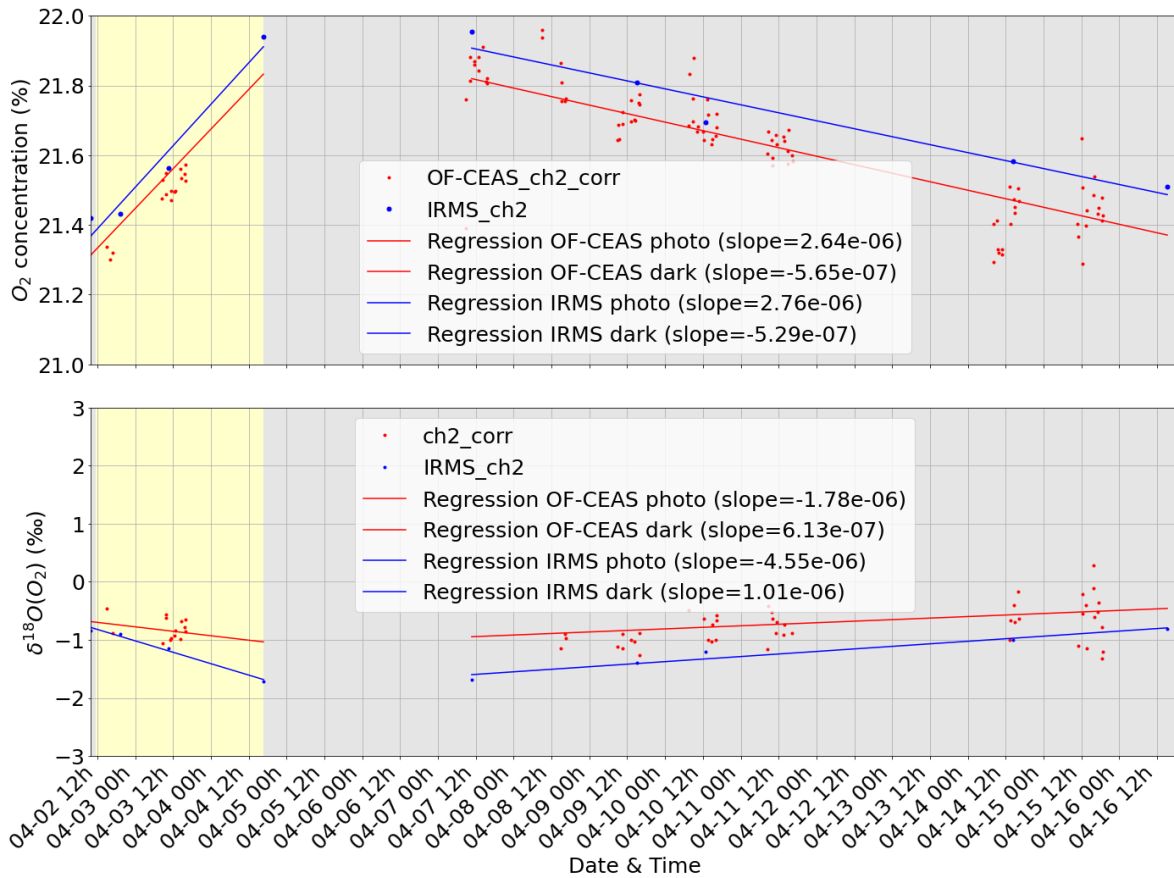


Figure S3: Comparison of the O₂ concentration (top panel, in %) and $\delta^{18}\text{O}(\text{O}_2)$ (bottom panel) measured by OF-CEAS (in red) and IRMS (in blue) for the light 5 and dark 6 phases of chamber 2. Note that due to high noise for OF-CEAS measurements, the regression lines are less reliable.

695

S3. Influence of a leak on the determination of the discrimination factor associated with respiration

We did a simple calculation to evaluate the possible influence of a leak from outside of the chamber on the determination of the discrimination factor associated with respiration.

700

- We first consider a base scenario of dark/respiration phase: O₂ decreases linearly in the chamber atmosphere with every time step, and as a result $\delta^{18}\text{O}(\text{O}_2)$ gradually increases as ¹⁶O is preferentially taken in by the algae with a given fractionation factor.
- We then model the same same scenario with the addition of a leak, characterised by a leak ratio, that mixes at each step the chamber atmosphere with external atmosphere characterised by fixed O₂ concentration and isotopic composition (21 % and $\delta^{18}\text{O}=0$ by definition). The results of these simulations are plotted in Fig. S4. When we calculate the $^{18}\text{E}_{\text{dark}}$ from the regression of $\ln(^{18}\text{R})$ vs $\ln(\text{O}_2)$, we do not find any significant impact of the leak.

705

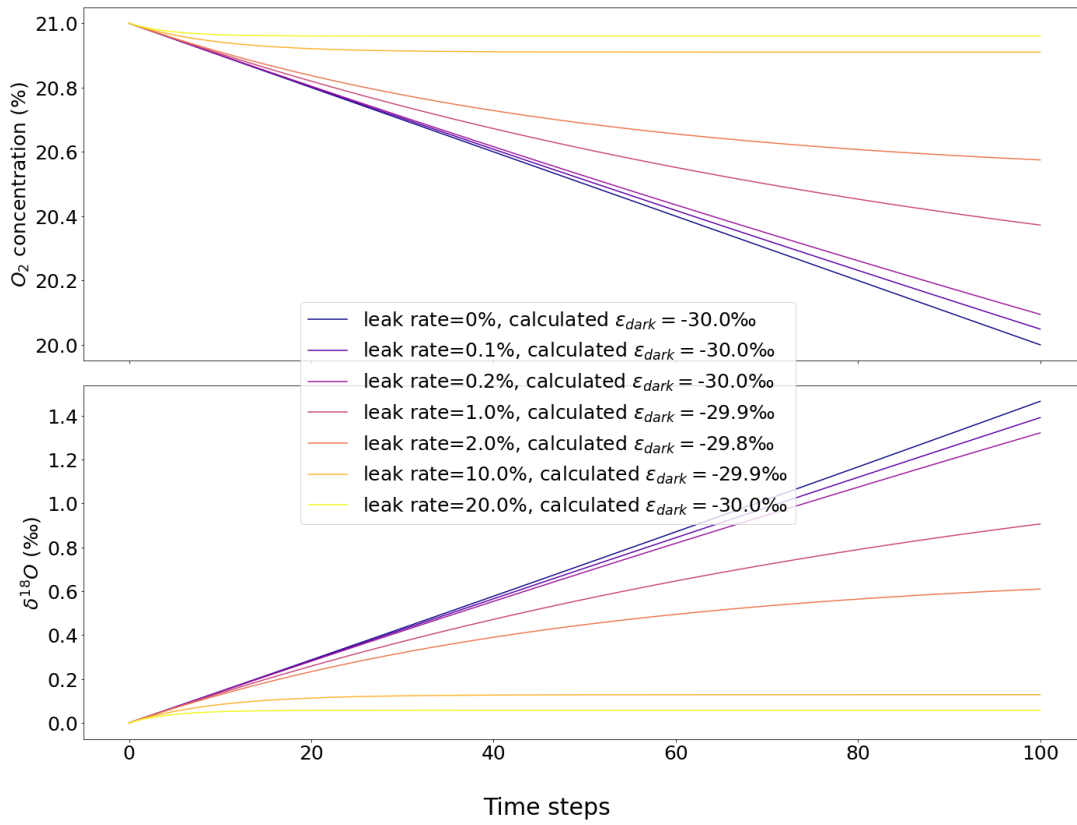


Figure S4: Results of the simulation of several leak rates (in legend) for a biological chamber: the evolution of O₂ concentration (top) and $\delta^{18}\text{O}(\text{O}_2)$ (bottom) during a dark/respiration only phase, and the calculated discrimination factors (in legend).